Journal: Hydrological Sciences Journal

Reference: HSJ-2015-0337

Paper title: Prediction of climate change effects on the runoff regime of a forested catchment in northern Iran

Authors: Farhad Hajian[1 †], Alan P. Dykes[2] *, Bagher Zahabiyoun[3] and Maia Ibsen [4]

Author affiliations:
[1]School of Civil Engineering and Construction (since renamed School of Natural and Built Environments), Kingston University, Penrhyn Road, Kingston upon Thames, KT1 2EE, UK.
f.hajian@yahoo.com
[2]Centre for Engineering, Environment and Society Research, School of Natural and Built Environments, Kingston University, Penrhyn Road, Kingston upon Thames, KT1 2EE, UK.
a.p.dykes@kingston.ac.uk
[3]Water Resources Engineering Group, School of Civil Engineering, Iran University of Science and Technology, Narmak, Tehran, PO Box 16765-163, Iran.
Bagher@iust.ac.ir
[4]Centre for Engineering, Environment and Society Research, School of Natural and Built Environments, Kingston University, Penrhyn Road, Kingston upon Thames, KT1 2EE, UK.
m.ibsen@kingston.ac.uk

[†]Present address: Department of Civil Engineering, Neyshabur Branch, Islamic Azad University, Neyshabur, Iran.

Correspondence: *Corresponding author (A P Dykes). Address and Email shown above.
Tel.: +44 (0)208 417 7018

Abstract: The southern coast of the Caspian Sea in northern Iran is bordered by a mountain range with forested catchments which are susceptible to droughts and floods. This paper examines possible changes to runoff patterns from one of these catchments in response to climate change scenarios. The HEC-HMS rainfall-runoff model was used with downscaled future rainfall and temperature data from 13 Global Circulation Models, and meteorological and hydrometric data from the Casilian (or ‘Kassilian’) Catchment. Annual and seasonal predictions of runoff change for three future emissions scenarios were obtained, which suggest significantly higher spring rainfall with increased risk of flooding and significantly lower summer rainfall leading to a higher probability of droughts. “Flash floods” arising from extreme rainfall may become more frequent, occurring at any time of year. These findings indicate a need for strategic planning of water resource management and mitigation measures for increasing flood hazards.

Key words: northern Iran, climate change, runoff modelling, weather generator, rainfall patterns

Prediction of climate change effects on the runoff regime of a forested catchment in northern Iran

Abstract

The southern coast of the Caspian Sea in northern Iran is bordered by a mountain range with forested catchments which are susceptible to droughts and floods. This paper examines possible changes to runoff patterns from one of these catchments in response to climate change scenarios. The HEC-HMS rainfall-runoff model was used with downscaled future rainfall and temperature data from 13 Global Circulation Models, and meteorological and hydrometric data from the Casilian (or 'Kassilian') Catchment. Annual and seasonal predictions of runoff change for three future emissions scenarios were obtained, which suggest significantly higher spring rainfall with increased risk of flooding and significantly lower summer rainfall leading to a higher probability of droughts. "Flash floods" arising from extreme rainfall may become more frequent, occurring at any time of year. These findings indicate a need for strategic planning of water resource management and mitigation measures for increasing flood hazards.

Key words: northern Iran, climate change, runoff modelling, weather generator, rainfall patterns

1 INTRODUCTION

There is increasing consensus from different GCMs that as the atmosphere continues to warm, rainfall intensity is likely to increase over many parts of the world with longer periods of very low rainfall in between and that increases in rainfall extremes are expected to be greater than the changes in mean precipitation (Easterling *et al*. 2000, Wilby and Wigley 2002, SWCS 2003, Kharin and Zwiers 2005, IPCC 2007). The mean air temperature near the surface of the earth increased by up to 0.35°C from the 1910s to the 1940s and by as much as 0.55°C from the 1970s to 2007 (IPCC 2007). For every 1°C increase in temperature, the water-holding capacity of the atmosphere will increase by about 7%, as predicted by the Clausius-Clapeyron equation which defines the vapour pressure curve for two-phase media (e.g. Venturini *et al*. 2008). Thus, a warmer climate may be expected to result in more rainfall but global climate models (GCMs) indicate more complex effects.

The type (e.g. convective, orographic, etc.), frequency, amount and intensity of rainfall are all predicted to change. If the frequency of dry days increases due to warming, this does not necessarily mean that the frequency of extreme rainfall events will decrease, depending on the threshold used to define such events (Barnett *et al*. 2006, IPCC 2007, Kundzewicz *et al*. 2013). With the increased water vapour in the atmosphere, more frequent and higher intensity rainfall events are likely to occur in many regions (Douville *et al*. 2002). High intensity rainfall, particularly if the total amount of storm rainfall is also very high as is often the case, commonly gives rise to short-duration, potentially high impact hazards such as flash floods. As a direct consequence of the changing rainfall patterns, landslides are also expected to increase in frequency. These constitute additional but related hazards that may be triggered by higher storm rainfall or, in the case of debris flows, caused by storm runoff in steep mountain streams entraining sediment. There are also signs that a higher incidence of prolonged droughts may be expected, especially in warmer climates. A series of Atmosphere-Ocean General Circulation Model (AOGCMs) simulations—run in advance of a 2008 IPCC report to represent the effects of a warmer climate—indicated a decrease in summer rainfall in most parts of the mid-latitudes (including Iran) and, thus, a greater risk of drought in these regions (Bates *et al*. 2008).

Northern Iran, comprising provinces that border the southern coastline of the Caspian Sea (Fig. 1), is susceptible to droughts and floods. Planning for improved water management for drought periods and infrastructure protection for floods is particularly important because it is one of

Iran's major tourist areas. Katiraei *et al*. (2007) found a trend of increasing annual rainfall totals over the period of 1960–2001 in the east of Mazandaran Province (significant at $p = 0.10$) and in 2001 there was a devastating flood in Golestan Province that resulted from a large rainfall event (>150 mm in 12 hours) of which the first hour was of very high intensity (50 mm h^{-1}) (Sharifi *et al*. 2012). Rainfall in the northern part of Iran mainly originates from southerly extensions of Siberian anticyclones. As high pressure develops over Siberia, elongated ridges of high pressure move to the north of Iran and pass over the Caspian Sea, receiving heat and humidity from the surface of the sea. The moist airflow moves south and rises as it hits the northern slope of the mountains, cooling and condensing to producing orographic precipitation. According to Rasoli *et al*. (2012), the Siberian high pressure system has decreased in strength in winter by up to 0.005 mb y^{-1} over a 61-year period (1948–2009). Therefore, the airflow from the north to the south of the Caspian Sea became weaker and transported less moisture, resulting in lower winter rainfall in northern Iran. However, the pressure of the central area of the Siberian high pressure in spring has increased by up to 0.059 mb y^{-1}, producing higher spring rainfall in northern Iran, generally of higher intensity, thus leading to an expectation of more floods in the southern Caspian Sea coastal area during the spring season (Rasoli *et al*. 2012). In parallel with the increasing rainfall, Tabari *et al*. (2011) found a significant annual trend of decreasing water levels in 190 observation wells in the east of Mazandaran Province during 1985–2007, although they did not explain the reasons for this trend. Possibilities include a higher proportion of convective rainfall which generates a higher runoff ratio and higher demand for abstracted groundwater from rising immigrant and tourist numbers.

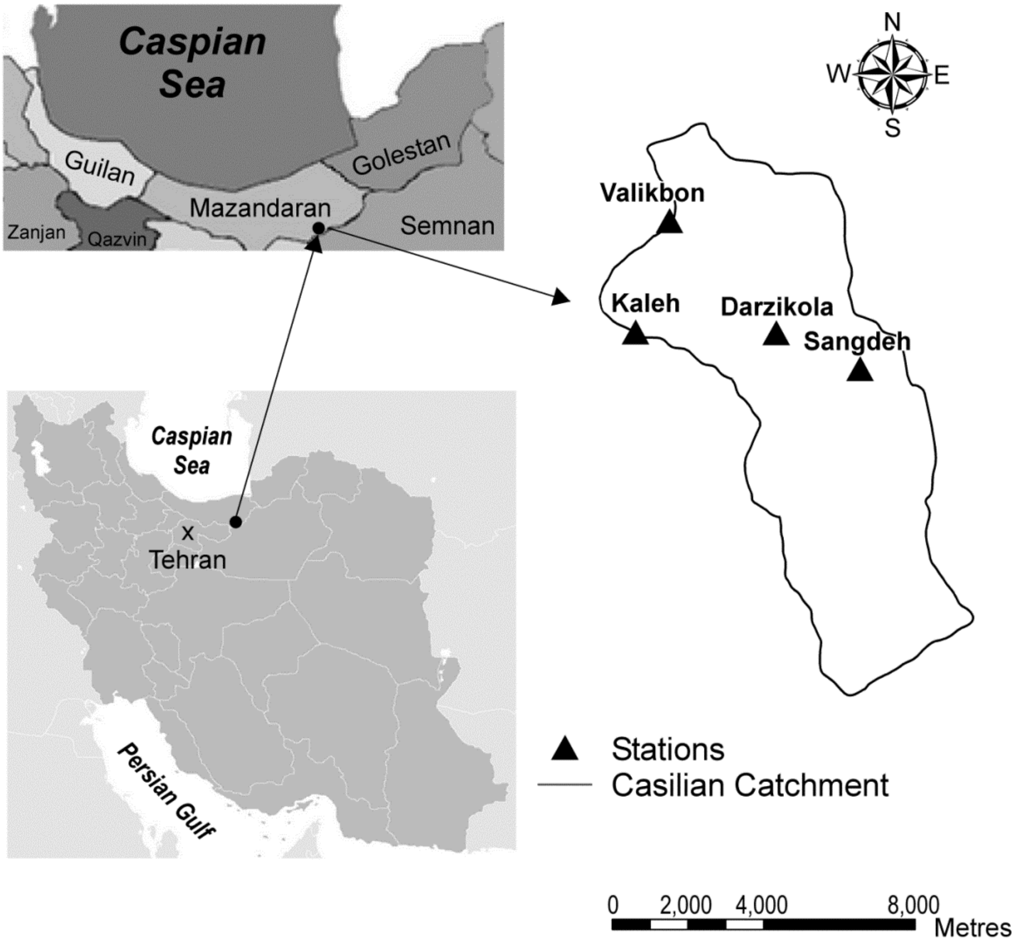

Figure 1. Location of the Casilian Catchment in Mazandaran Province, northern Iran, showing locations of hydrometric monitoring stations within the catchment. Valikbon station defines the outflow from the study catchment.

Long-term changes to runoff regimes and groundwater resources have also been observed in many other parts of the world. For example, Banasik and Hejduk (2012) found a trend of decreasing annual runoff from a small catchment in Poland over a 48-year period with no apparent cause, in that there had been no precipitation trend and no human interventions. However, other recent studies have distinguished the influence of climatic variations from the more tangible evidence of anthropogenic modification of catchments and increasing utilisation of available water resources. Chang *et al*. (2015) found that in the large catchment of the Weihe River in northwest China, a declining trend in annual runoff was associated with reducing precipitation during 1956-70 but that after 1970 human activities had twice as much influence on the continuing runoff reductions; similarly, the contributions of human activities was three times higher since 1990 in the Wei River basin in China (Zhan *et al*. 2014). Regionally, it becomes more difficult to explain runoff trends as there may be complex interactions between different factors in different parts of a region or even different subcatchments of a large river basin, especially if some rivers show long-term increases in annual runoff (e.g. in some European countries: Stahl *et al*. 2010) while in others the runoff is seen to be reducing (e.g. Li *et al*. 2014, Jiang *et al*. 2015), and seasonal changes may be more significant in magnitude and potential impact than annual trends (Stahl *et al*. 2010). Even at much smaller spatial scales, if additional natural factors such as snowmelt or significant groundwater storage contribute to the overall hydrological response of a catchment, it becomes increasingly difficult to separate climatic effects from human activities (e.g. Langhammer *et al*. 2015). Predictions of future runoff trends resulting from different land use or catchment management scenarios ultimately require adequate understanding of possible climatic patterns and corresponding runoff responses. This study addresses the topic from the latter perspective.

The aim of this paper is to use outputs from General Circulation Models (GCMs—often referred to as “global climate models”) to identify and characterise possible future changes in the runoff regimes of forested catchments in northern Iran that drain into the Caspian Sea along its southern coastline. Runoff for future climate scenarios was estimated using a publicly available catchment runoff model. The working hypothesis is that runoff regimes will show significant changes compared with the present, with the direction of change (i.e. increasing or decreasing runoff) varying both annually and seasonally in line with the rainfall trends identified in recent decades. Implications of the results for future water management are identified and discussed.

2 STUDY SITE

This research focused on the Casilian Catchment (also known in Iran as Cassilian, Kasilian or Kassilian Catchment) in Mazandaran Province, northern Iran (53°18’ to 53°30’E and 35°58’ to 36°07’N) (Fig. 1). This catchment was selected because the data availability was far greater than for other areas. Tamab, Iran’s Water Resources Research Organization based in Tehran, collect basic climate (rainfall and temperature) and runoff (discharge and sediment) data for many catchments in Iran (Parvardeh 1985). The data used for this research were originally provided by the Head of Tamab’s Surface Water Section, J. Parvardeh, to BZ for research on Casilian Catchment. The study area within this catchment is bounded to the north by the Setic and Chartab mountains with heights of up to 1790 m and to the south by the Mirozad (2700 m) and Golrad (3349 m) mountains. To the west is the Getoja Mountain (2043 m) and to the east is the Chartab Mountain (1613 m). The main river drains northwards, eventually discharging into the Caspian Sea. The study area is defined as the upper 65.7 km^2 of the catchment upstream of Valikbon hydrometric station (see below) at 1120 m elevation. Most of the upper tributaries extend to the southern rim of the catchment at around 3000–3300 m elevation. The longest flow path, representing the catchment length, is 17.8 km. Indicative mean channel gradients are 0.5 for the first two kilometres of the upper tributaries down the steep escarpment that defines the southern edge of the catchment, then 0.057 for the next 15.8 km. Approximately 80% of the catchment is forested, the upstream (southern) half of the catchment comprising high quality forest that could theoretically be susceptible to significant deforestation in the future. Most of the downstream area of the catchment has been cleared for agriculture (crops and pasture) and there are several small villages. The geology of the catchment is dominated by shale, sandstone, marl and siltstone.

There are two meteorological stations (Darzikola and Sangdeh), one rainfall station (Kale) and one hydrometric station (Valikbon) in the Casilian Catchment (Fig.1). Sangdeh station, located at the southeast end of Sangdeh village, records daily rainfall and daily temperatures. Darzikola station only records daily rainfall data, as does Kale station. The Valikbon hydrometric station, on the Casilian River, is located near to Valikbon village and records the discharge from the upper catchment that comprises the study area.

The mean annual rainfall on the Casilian Catchment for the 20-year period 1977–1996 was estimated to be around 756 mm, using Thiessen polygons (McCuen 1998) formed around the three rainfall stations. Monthly mean rainfall varies throughout the year from around 48 mm in December (minimum) to 89 mm in August (maximum). The mean annual runoff from 13 full years between 1980 and 1996 for which complete discharge data exist was 229 mm. The mean runoff ratio for these 13 years was 0.27. However, the runoff ratio for March and April (61 days) was highly variable across the 13 years of data, exceeding 1.0 in 1980 (1.34) and 1982 (2.00). We interpret this as demonstrating a major snowmelt contribution to the runoff regime (after Zampieri *et al*. 2015). According to Tamab, snowfall on this catchment is negligible. However, it is likely that the Tamab data and residents' comments are referring to snow at Sangdeh and further downstream. As is the case on the mountains along the northern side of Tehran we think that there is significant snowfall most winters on the high mountains upstream of Sangdeh where people rarely go and where there are no monitoring facilities.

3 METHODOLOGY

We obtained the most complete set of catchment hydrometric data for northern Iran that was available from Tamab, which was for the Casilian Catchment (Parvardeh 1985). The outline strategy for this research was to use downscaled GCM climate data for three future periods of the 21st century and three global emissions scenarios as the input data for estimating total runoff volumes from the catchment using a suitable rainfall-runoff model. GCM data were downscaled using a Weather Generator (WG). The simulations were performed for mean annual conditions and for seasonal conditions.

3.1 Field data

Daily precipitation and temperature data for the Casilian Catchment were obtained at Sangdeh for the period 23 September 1976 to 22 September 1997, but with some missing data. Discharge data from Valikbon were available for the periods 23 September 1979 to 22 September 1987, 23 September 1988 to 22 September 1993 and 23 September 1994 to 22 September 1998. The incomplete discharge record limited the durations of time periods that could be utilised for this study. The longest continuous complete record included calendar years 1980–86 inclusive. This 7-year period was thus designated the "baseline" period and its discharge regime is summarised in Table 3.

The accuracy and reliability of the recorded field data are not known and cannot be verified. Three of the authors of this paper (FH, APD, BZ) visited Sangdeh meteorological station and Valikbon hydrometric station on 24 May 2010 and were able to inspect the equipment and verify recording procedures with one of the station operators. As a result we are confident that the Sangdeh data are probably reliable but there are thought to be some systematic errors in the data from Valikbon resulting in proportionally larger errors as the discharge reduces (J. Parvardeh, Tamab, pers. comm.). For the purposes of this study, however, any errors and inaccuracies in the input data will not materially affect the generalised results and interpretations of the modelling analyses.

Table 3. Summary of the runoff regime at Valikbon station in the Casilian Catchment. All values are discharges in cubic metres per second. Source: Tamab.

SEASON	DISCHARGE	1980	1981	1982	1983	1984	1985	1986	MEAN
Autumn	highest peak	3.23	4.17	2.04	3.34	2.85	1.70	0.56	–
	mean	0.41	0.40	0.44	0.34	0.29	0.22	0.11	0.32
Winter	highest peak	2.22	3.46	1.78	4.15	6.25	2.20	no data	–
	mean	0.68	0.66	0.45	0.85	0.77	0.40		0.64
Spring	highest peak	3.00	4.76	1.96	2.75	3.62	2.71	4.29	–
	mean	0.47	0.63	0.59	0.73	0.71	0.43	0.74	0.64
Summer	highest peak	1.92	5.75	3.63	13.87	1.88	0.73	0.66	–
	mean	0.17	0.55	0.24	0.79	0.21	0.09	0.04	0.30

3.2 Climate data for future scenarios

Different GCMs have been developed in various countries of the world. For a given emissions scenario, each GCM can be used to predict patterns of temperature and rainfall change for a region of the Earth's surface (Kay *et al*. 2009). However, GCM outputs cannot be used directly for a specific site of interest due to their coarse scale: even in a high resolution GCM, one grid box represents an area of greater than 50 000 km^2 (Semenov *et al*. 1998). One method by which GCM data can be used for small areas is to downscale the climate predictions using a "weather generator". This is a model that can produce synthetic weather data for continuous periods, e.g. daily rainfall for several years, according to the statistical properties of present rainfall at a location of interest that are modified by a proportion indicated by the GCM output.

We used the Long Ashton Research Station Weather Generator (LARS-WG) for this study because it is readily available for use and its performance is regarded as being superior to that of other WGs such as WGEN and Artificial Neural Network models (Semenov *et al*. 1998, Sajjad *et al*. 2006). LARS-WG was used to downscale the Global Climate Model (GCM) outputs to the area around Sangdeh Station to overcome the limitations of the coarse scale GCM output. A new version, LARS-WG 5, generates rainfall and temperature data for 20-year periods 2011–2030, 2046–2065 and 2080–2099 for 13 climate models and three scenarios, having specified the longitude, latitude and altitude of the station used to provide the statistics of the observed weather data. The performance of this WG was evaluated by entering the daily rainfall and daily maximum and minimum temperatures recorded at Sangdeh station from 1 January 1977 to 31 December 1996 inclusive. The software calculated the monthly mean and monthly standard deviation of these parameters and then used these statistics to generate 300 years-worth of daily values (e.g. Semenov *et al*. 1998, Sajjad *et al*. 2006). It then compared these statistical properties for the original and the generated daily rainfall data using the t-test and the F-test. For both tests $p < 0.05$ indicating that the means of the observed and synthetic monthly rainfall totals, and the standard deviations of the two sets of monthly rainfall for each month, were not significantly different. Mean monthly minimum and mean monthly maximum temperatures of the observed and generated data for all months were identical, with only slight differences between the respective standard deviations.

To investigate the climate change effects on runoff from the Casilian Catchment, climate data representing the effects of different climate change scenarios were required as inputs for the rainfall-runoff model. Five different sources of uncertainty exist in climate change impact studies: (i) future greenhouse gas emissions; (ii) GCM structure; (iii) downscaling from GCMs; (iv) hydrological model structure; (v) hydrological model parameters (Kay *et al*. 2009, p.1). The uncertainty related to the choice of GCM is greater than that from the other sources of uncertainty

(Bates *et al*. 2008, Kay *et al*. 2009, Boyer *et al*. 2010, Bae *et al*. 2011). GCMs contain significant uncertainties and IPCC (2007) recommended that the results of different climate models and scenarios should be considered in climate change studies (Abbaspour *et al*. 2009). Thirteen climate models (BCM2, CNCM3, CSMK3, FGOALS, GFCM21, GIAOM, HADCM3, HADGEM, INCM3, IPCM4, NCCCSM, NCPCM and CGMRS) and three emissions scenarios (A1B, A2 and B1) that are available in LARS-WG provide different projections and produce different magnitudes and patterns of rainfall and temperature changes.

Using the same observed data as for the evaluation, above, plus the coordinates of Sangdeh station, LARS-WG produced daily rainfall and temperature data from all 13 models for three 7-year periods (2011–2017, 2046–2052 and 2080–2086). All simulations and analyses in this study use 7-year periods because the baseline period 1980–86 (inclusive) is the longest complete record of discharge in the field data. The range of uncertainty in the GCM predictions (King *et al*. 2009, Semenov and Stratonovitch 2010, Semenov and Shewry 2011) is indicated in Fig. 2 for annual rainfall totals, the boxplots representing the 25th, 50th (median) and 75th percentiles of the outputs from the thirteen GCMs with the full (1977–96 inclusive) and baseline sets of observed data superimposed. Predicted annual rainfall totals are shown for each future simulation period under the influence of each emissions scenario. Fig. 3 shows a similar variability of results for GCM predictions of the number of days in each 7-year period with "heavy rainfall", defined as daily rainfall >95th percentile (IPCC 2007, King *et al*. 2009). In this study the 95th percentile from all non-zero rainfall events for 1980–86 is 18 mm d^{-1}, which occurred on 50 days within this period (i.e. seven days per year on average). The frequency of such heavy rainfall events is predicted to increase for all future periods and scenarios in comparison with the baseline observed data.

3.3 Catchment rainfall-runoff modelling

We used the HEC-HMS rainfall-runoff model for this research. HEC-HMS is the "Hydrological Modelling System" developed by the Hydrologic Engineering Centre of the US Corps of Engineering and has been used successfully for many types of investigations in different parts of the world (Cunderlik and Simonovic 2005). It is one of several rainfall-runoff modelling systems developed in recent years and made available for application to a wide range of hydrological issues, including investigation of the possible effects of global climate change on the hydrological processes of a catchment.

HEC-HMS comprises two main components: a catchment model and a meteorological model, the latter determining the net inputs to the subsurface hydrological system resulting from the weather patterns experienced by the study location. Critical to this is the determination of the mean monthly potential evapotranspiration (PET). The meteorological model incorporates the Penman–Monteith method, which requires temperature, wind speed, solar radiation and relative humidity data (Bae *et al*. 2011), and the Thornthwaite method which only needs temperature data (Mahdavi 2004). The latter was used in this study because only temperature data exist for the Casilian Catchment. This was not considered a significant limitation because uncertainties in PET estimation tend to have smaller effects on simulated runoff in climate change impact studies than the uncertainties arising from the type of GCM or the future climate scenario (e.g. Bae *et al*. 2011). HEC-HMS can also calculate runoff responses to snowfall but this requires data that do not exist for the Casilian Catchment including snowpack characteristics and parameters that control melting (e.g. solar radiation and dew point temperature). Consequently, it was considered unfeasible to attempt to model snowfall for this study.

The catchment model incorporates three rainfall-runoff transformation processes. The first of these calculates the volume of runoff from a catchment as being the proportion of rainfall remaining in the system after "losses" have been subtracted. This is done using a 5-layer Soil Moisture Accounting (SMA) procedure which estimates the losses to interception, infiltration, percolation and deep percolation and subtracts them from the precipitation. These losses contribute to canopy-interception storage, surface-depression storage, soil-profile storage and one or two

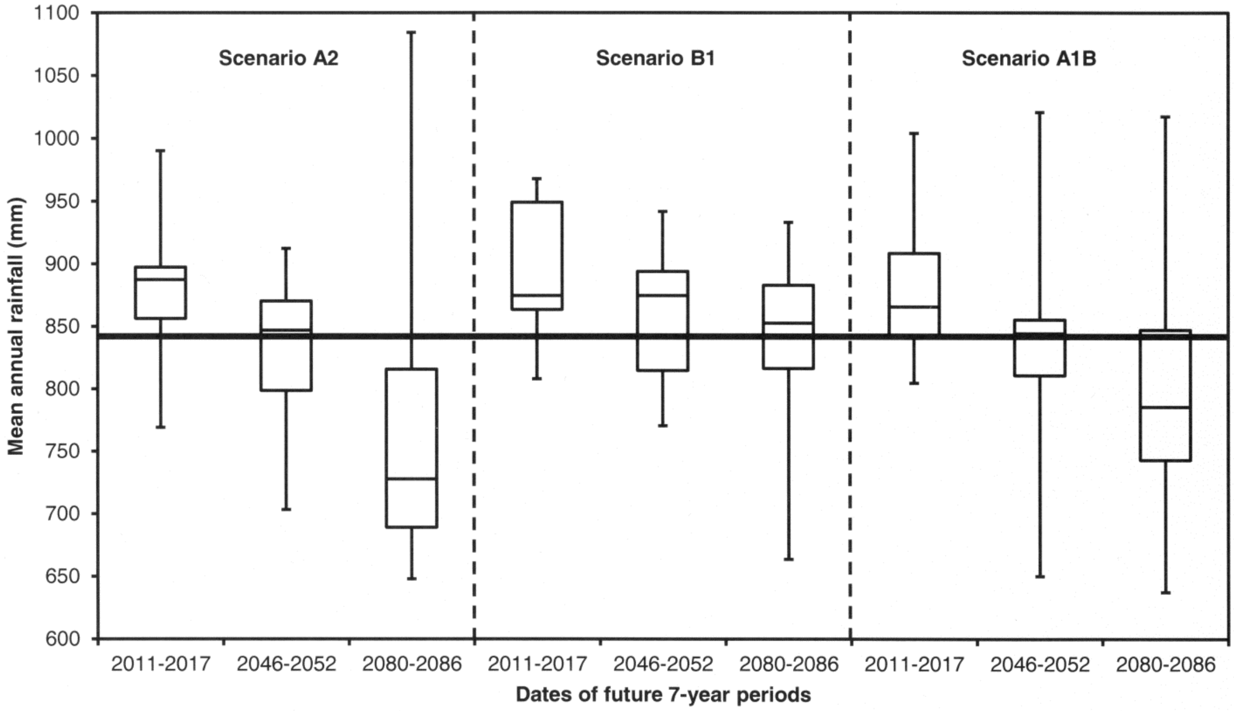

Figure 2. Variations in future annual rainfall projections for the Casilian Catchment produced by LARS-WG shown as boxplots (maximum, minimum, median, upper and lower quartiles of the mean annual values produced by 6-13 GCMs). The horizontal line represents the mean annual rainfall for both reference periods (2.0 mm difference).

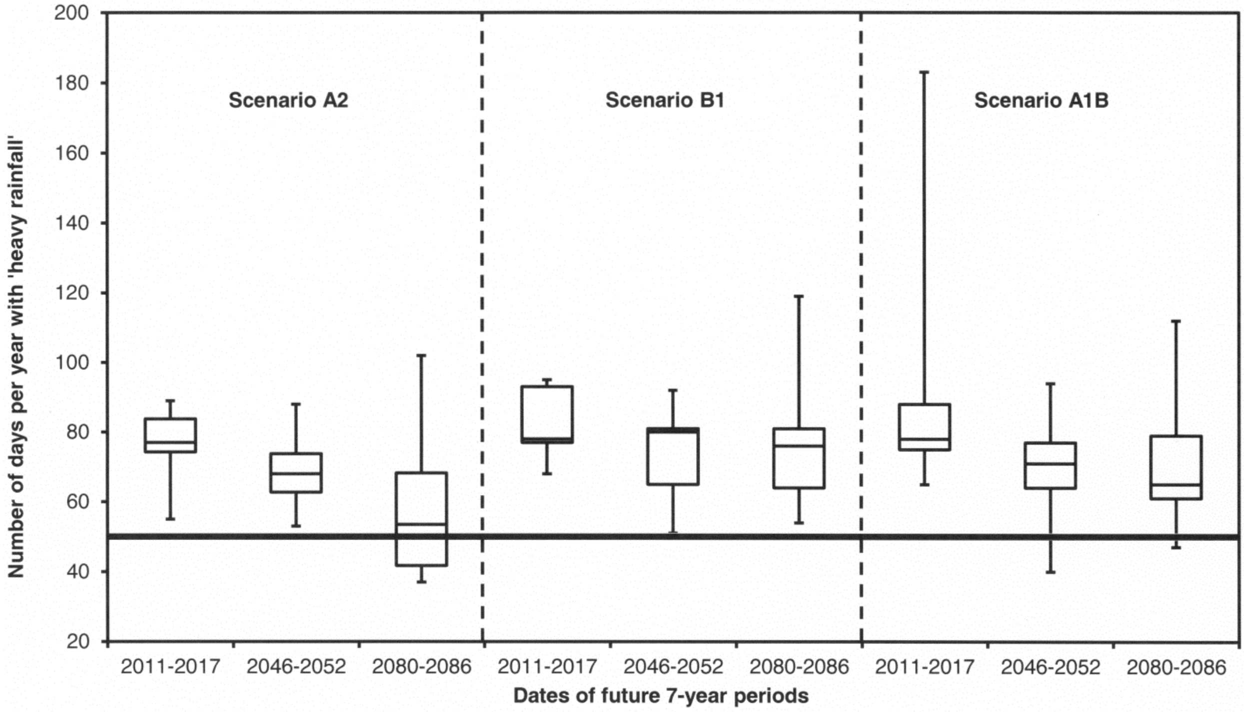

Figure 3. Variations in future projections of the number of days with "heavy rainfall", i.e. >95th percentile of the observed base period, within each 7-year period for the Casilian Catchment produced by LARS-WG shown as boxplots (details as in Fig. 2). The horizontal line represents the number of such wet days recorded during the baseline period 1980-86 inclusive.

layers of groundwater storage (Cunderlik and Simonovic 2005). The output from the SMA procedure contributes to the other two transformation processes, direct runoff and groundwater flow. The direct runoff (i.e. channel discharge) is modelled using the SCS (Soil Conservation Service) dimensionless unit hydrograph and the groundwater flow is transformed into base flow by a linear reservoir base flow (LRBF) method that was designed to integrate with the SMA procedure (USACE-HEC 2000).

To model the hydrological processes in a catchment, HEC-HMS requires values for 23 parameters. Most parameters of the catchment model need only an initial estimate, their final values being obtained through automated optimisation using the "Nelder Mead" search method. The estimated parameter values are adjusted until the value of the selected objective function—in this case the goodness-of-fit between the observed and computed total runoff volume from the catchment—is minimized (Scharffenberg and Fleming 2010). For this study, initial values for all 23 parameters (listed in Table 1) were obtained from geology, soil and land use maps and from published sources (Rawls *et al*. 1982, USDA 1986, Bennett 1998, McCuen 1998, Singhal and Gupta 1999, Chainuvati and Athipanan 2001, Breuer *et al*. 2003, Fleming and Neary 2004, Garcı´a *et al*. 2008, McEnroe 2010). A standard calibration–validation procedure was then followed (as initially set out in Section 2.1 of Trucano *et al*. 2006), with parameter optimisation taking place within the calibration stage.

4 RESULTS

4.1 Model calibration and validation

Calibration of the catchment model was performed for two different rainfall inputs, using: (i) the mean rainfall of three stations (Sangdeh, Kale and Darzikola) calculated by the Thiessen method, and (ii) the rainfall recorded at Sangdeh rainfall station only, to determine which option appeared to correspond more closely with the observed runoff patterns. Observed rainfall and temperature data were first entered into the meteorological model in order to determine the mean monthly PET, then the catchment model was run and its calculated discharge was compared with the observed discharge. The percentage error in the calculated annual runoff volume was designated as the objective function for this and all subsequent model runs because this study is concerned with future changes to runoff regimes:

$$\%\ \text{error}\ (R_v) = (SR_v - OR_v) / OR_v \qquad (1)$$

where R_v is the runoff volume, "S" indicates "simulated" and "O" is "observed". The calibration was performed as a "continuous" simulation using rainfall, temperature and discharge data for the period 1 January 1980 to 31 December 1986 inclusive and the smallest error, 4.8%, was obtained from parameter values optimised for rainfall at Sangdeh station only (Table 1). These optimised parameter values and Sangdeh rainfall data were therefore used to validate the catchment model using observed data from 1 January 1989 to 31 December 1992 inclusive; the resulting error of 4.9% was considered acceptable. These periods of observed data were used because they comprise the most complete parts of the data record.

The performance of HEC-HMS was evaluated further by performing the same calibration–validation simulations for each season separately, following Iran's water year, but using the optimised parameter values from the main calibration exercise. The runoff volumes for each season were extracted from the full calibration and validation simulations and compared with the corresponding runoff volumes recorded at Valikbon. Table 2 shows that for half of the year the optimised parameter values do not produce very accurate results, which suggests that there are some significant seasonal controls operating in the catchment. A strong possibility is that winter precipitation is actually snow that accumulates rather than contributing to runoff, and that some

Table 1. Initial estimates of parameter values in HEC-HMS for calibration of the "continuous" model after optimisation using the "Nelder Mead" search method and rainfall data from Sangdeh station.

PARAMETER	UNITS	VALUE FOR "CONTINUOUS" MODEL
Canopy storage	mm	1.2
Surface storage	mm	1.0
Maximum soil infiltration rate	mm h^{-1}	50.1
Impervious area	%	3.6
Soil storage	mm	125.0
Lag time	min	1007.0
Tension storage	mm	15.0
Soil percolation rate	mm h^{-1}	6.1
Initial canopy storage	%	20.0
Initial surface storage	%	20.0
Initial soil storage	%	30.0
Initial groundwater 1 (GW1) storage	%	40.0
GW1 storage	mm	7.0
GW1 percolation	mm h^{-1}	0.7
GW1 coefficient	h	50.2
GW1 initial discharge (linear reservoir)	m^3 s^{-1}	0.5
GW1 coefficient (linear reservoir)	h	50.2
Initial groundwater 2 (GW2) storage	%	40.0
GW2 storage	mm	7.0
GW2 percolation	mm h^{-1}	0.7
GW2 coefficient	h	50.2
GW2 initial discharge (linear reservoir)	m^3 s^{-1}	0.0
GW2 coefficient (linear reservoir)	h	50.2

Table 2. Percent error in simulated runoff volumes for the full year and seasonal calibration and validation periods.

CALIBRATION		VALIDATION	
Full year, 7 years 1 Jan. 1980 to 31 Dec. 1986	4.8%	Full year, 4 years 1 Jan. 1989 to 31 Dec. 1992	4.9%
CALIBRATION PERIOD (CALIBRATED)		VALIDATION PERIOD (CALIBRATED)	
Autumn, 7 years 23 Sep.–21 Dec. only	7.4%	Autumn, 4 years 23 Sep.–21 Dec. only	4.9%
Winter, 7 years 22 Dec.–20 Mar. only	32.7%	Winter, 4 years 22 Dec.–20 Mar. only	14.3%
Spring, 7 years 21 Mar.–21 Jun. only	21.8%	Spring, 4 years 21 Mar.–21 Jun. only	19.9%
Summer, 7 years 22 Jun.–22 Sep. only	5.2%	Summer, 4 years 22 Jun.–22 Sep. only	3.7%

runoff in spring is from snowmelt that does not correspond with any rainfall. The fact that the calibrated model performs better against the validation data than against the calibration data for all seasons separately may reflect inherent differences between the two datasets, such as larger seasonal contrasts during the calibration period that would be smoothed somewhat by the model calibration. Furthermore, we consider it very likely that some catchment parameter values vary seasonally, particularly (mean) canopy storage relating to the deciduous tree cover but also soil infiltration rate and soil storage, which will both be zero if the ground is frozen.

The absence of data relating to snowfall or the possible duration and spatial extent of freezing conditions in the upper catchment precluded rigorous seasonal optimisation of the model for this study. However, we did set out to explore the possible seasonal changes to runoff that may arise in the future. Consequently we proceeded by using the calibrated parameters obtained from annual optimisation, recognising that the seasonal results that we present must be interpreted with caution but that they may nevertheless indicate temporal patterns that should be considered in any future water management planning for the region.

4.2 Runoff simulations for future rainfall scenarios

Different climate models represented within LARS-WG each provide projections for every climate scenario in terms of patterns of rainfall and temperature. The number of GCM outputs for each scenario and future 7-year period is shown in Table 4. The variations in these outputs are shown in Figs. 2 and 4. Fig. 4 shows the mean annual temperature already higher than the reference periods (1980–86 or 1977–96) and increasing significantly from each 7-year period to the next in all scenarios, though less dramatically for scenario B1. Fig. 2 indicates decreasing annual rainfall throughout the century but with higher inter-annual variability towards the end of the century. Again, this general trend is not as strong for scenario B1. However, the annual rainfall totals are suggested to be initially higher than recorded during either reference period but falling to lower levels later.

Table 4. Number of GCMs producing climate outputs for the dates and scenarios considered in this study.

	A2	B1	A1B
2011-17	8	9	13
2046-52	8	9	13
2080-86	6	9	11

Table 5. Mean projected changes in annual rainfall (% of reference period values) and annual temperature (°C) from LARS-WG and corresponding annual runoff (% of reference period values) simulated by HEC-HMS.

Scenario:	A2			B1			A1B		
Dates:	2011-17	2046-52	2080-86	2011-17	2046-52	2080-86	2011-17	2046-52	2080-86
Reference period	Percent change in annual rainfall								
1980-86	5.2	0.4	-13.7	3.7	3.7	1.1	2.6	0.1	-6.9
1977-96	5.4	0.6	-13.5	3.9	3.9	1.3	2.9	0.3	-6.6
	Change in annual temperature (°C)								
1980-86	1.3	2.4	4.5	1.0	1.7	2.1	1.0	2.4	3.6
1977-96	1.2	2.3	4.4	0.9	1.6	2.0	0.9	2.3	3.5
	Percent change in annual runoff								
1980-86	4.1	-1.5	-20.6	3.4	2.7	-1.6	1.8	-2.8	-12.7

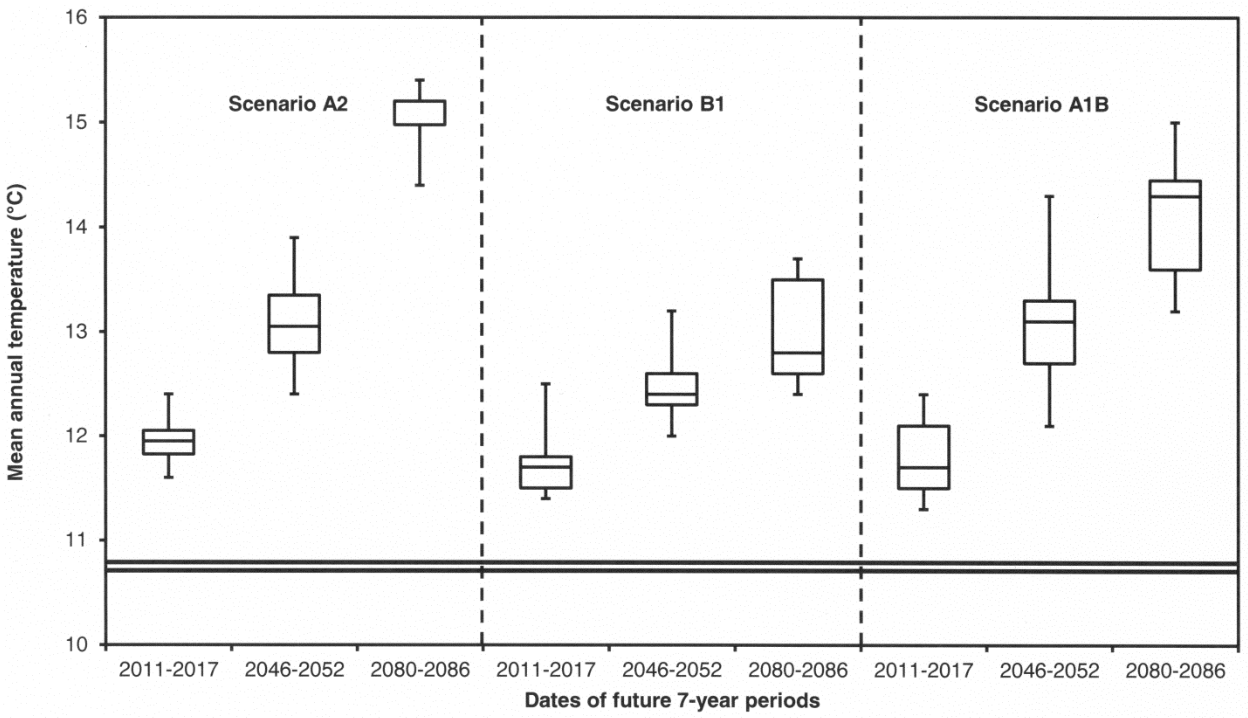

Figure 4. Variations in future annual temperature projections for the Casilian Catchment produced by LARS-WG shown as boxplots (details as in Fig. 2). The upper horizontal line shows the mean annual temperature for the 1977-96 reference period and the lower line represents the same for 1980-86 (0.1°C difference).

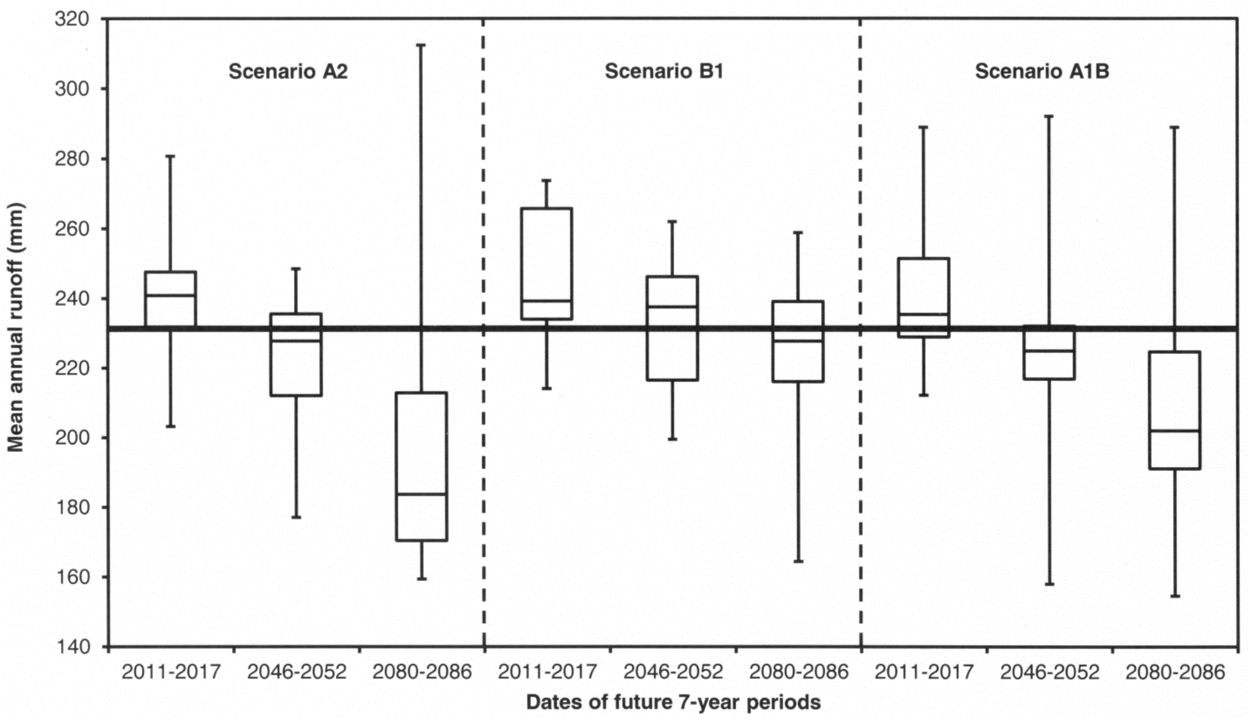

Figure 5. Variations in future annual runoff for the Casilian Catchment simulated by HEC-HMS shown as boxplots (details as in Fig. 2). The horizontal line represents the mean annual runoff for the baseline period 1980-86.

The median changes in rainfall and temperature obtained from the GCMs and the corresponding changes in annual runoff calculated by HEC-HMS are indicated in Table 5 as percentages of the mean values for the two reference periods. These annual runoff variations are illustrated in terms of depth-equivalent runoff in Fig. 5. The patterns of projected runoff variations are very similar to the patterns of projected annual rainfall totals. Table 6 shows the seasonal changes as percentages of the mean values for the two reference periods. These results for winter and spring must be considered uncertain for reasons identified earlier, although the increasing temperatures may result in less of the winter (and spring) precipitation falling as snow with less of a delay between precipitation and (snowmelt) runoff. However, the results in Table 6 were obtained with no representation of snow and subsequent melting yet still show significantly higher mean runoff in spring, an effect that may be further exaggerated by melting of winter snow and has been highlighted by Rasoli *et al*. (2012) as an effect of the changing Siberian high pressure. The predicted reduction in mean runoff in summer compared with the reference period is similarly marked but also somewhat more reliable, notwithstanding the caveats discussed previously.

Table 5. Mean projected changes in annual rainfall (% of reference period values) and annual temperature (°C) from LARS-WG and corresponding annual runoff (% of reference period values) simulated by HEC-HMS.

Scenario:	A2			B1			A1B		
Dates:	2011-17	2046-52	2080-86	2011-17	2046-52	2080-86	2011-17	2046-52	2080-86
Reference period	Percent change in annual rainfall								
1980-86	5.2	0.4	-13.7	3.7	3.7	1.1	2.6	0.1	-6.9
1977-96	5.4	0.6	-13.5	3.9	3.9	1.3	2.9	0.3	-6.6
	Change in annual temperature (°C)								
1980-86	1.3	2.4	4.5	1.0	1.7	2.1	1.0	2.4	3.6
1977-96	1.2	2.3	4.4	0.9	1.6	2.0	0.9	2.3	3.5
	Percent change in annual runoff								
1980-86	4.1	-1.5	-20.6	3.4	2.7	-1.6	1.8	-2.8	-12.7

5 DISCUSSION

Predicted changes to annual runoff from the Casilian Catchment correspond predictably with emissions scenarios. Scenario A2 represents slow global economic convergence with corresponding increasing demand for energy and materials and slow development of more efficient and non-fossil energy sources (IPCC 2000), i.e. the worst of the three represented in this study. Using all available GCMs for the selected future periods of time and emissions scenarios incorporated into LARS-WG, we have found that this scenario gives rise to more warming (Fig. 4) and the greatest reductions in mean annual rainfall (Fig. 2) and, thus, runoff (Fig. 5) towards the end of the present century. Likewise scenario B1 which represents the most optimistic case—rapid catch-up of less developed regions but with reduced energy demand and more rapid expansion of renewable supplies (IPCC 2000)—shows the smallest changes with perhaps a very small reduction in mean annual runoff by the 2080s. Predictions arising from scenario A1B, representing a more “balanced” pattern of global changes between A2 and B1, fall between these extreme cases. These are, of course, very broad generalisations that hide much variability and uncertainty. The variability among the rainfall predictions from the different GCMs is illustrated in Fig. 2, but this integration of the different predictions serves to reduce the degree of uncertainty inherent in each individual GCM output (King *et al*. 2009, Semenov and Stratonovitch 2010, Semenov and Shewry 2011).

Table 6. Mean projected changes in seasonal rainfall (% of reference period values) and temperature (°C) from LARS-WG and corresponding seasonal runoff (% of reference period values) simulated by HEC-HMS: (a) autumn, (b) winter, (c) spring, (d) summer. In all cases, the mean value for each season from all years in the respective data period is compared with the corresponding mean value for each season from all years in each simulation period.

(a)	A2			B1			A1B		
	2011-17	2046-52	2080-86	2011-17	2046-52	2080-86	2011-17	2046-52	2080-86
Ref. period	Percent change in autumn rainfall								
1980-86	6.3	10.1	2.5	5.1	2.2	4.8	4.1	3.8	-3.8
1977-96	11.5	15.4	7.5	10.2	7.1	9.9	9.1	8.9	0.8
	Change in autumn temperature (°C)								
1980-86	1.4	2.4	4.3	0.9	1.8	2.3	1.3	2.3	3.4
1977-96	4.2	5.2	7.1	3.7	4.6	5.1	4.1	5.1	6.2
	Percent change in autumn runoff								
1980-86	3.8	10.0	-1.1	5.6	1.2	2.9	2.6	3.1	-8.2

(b)	A2			B1			A1B		
	2011-17	2046-52	2080-86	2011-17	2046-52	2080-86	2011-17	2046-52	2080-86
Ref. period	Percent change in winter rainfall								
1980-86	1.2	0.0	0.4	-0.9	1.2	-3.9	-0.2	-0.3	-1.9
1977-96	-2.6	-3.8	-3.4	-4.6	-2.6	-7.5	-3.9	-4.0	-5.5
	Change in winter temperature (°C)								
1980-86	0.9	1.9	3.4	0.6	1.5	1.6	0.7	1.9	2.7
1977-96	3.9	4.9	6.4	3.6	4.5	4.6	3.7	4.9	5.7
	Percent change in winter runoff								
1980-86	1.2	-2.3	-3.0	-2.3	-0.8	-4.8	-2.0	-2.1	-4.1

(c)	A2			B1			A1B		
	2011-17	2046-52	2080-86	2011-17	2046-52	2080-86	2011-17	2046-52	2080-86
Ref. period	Percent change in spring rainfall								
1980-86	18.5	9.7	-7.5	22.1	13.3	12.8	17.7	11.2	-0.1
1977-96	7.9	-0.1	-15.8	11.1	3.1	2.6	7.1	1.2	-9.1
	Change in spring temperature (°C)								
1980-86	1.2	2.5	4.6	1.0	1.8	2.3	1.0	2.5	3.4
1977-96	4.3	5.6	7.7	4.1	4.9	5.4	4.1	5.6	6.5
	Percent change in spring runoff								
1980-86	32.3	14.2	-5.3	32.4	22.6	18.8	25.9	18.6	3.8

(d)	A2			B1			A1B		
	2011-17	2046-52	2080-86	2011-17	2046-52	2080-86	2011-17	2046-52	2080-86
Ref. period	Percent change in summer rainfall								
1980-86	-12.9	-20.4	-31.1	-8.6	-10.2	-14.9	-11.1	-19.1	-22.3
1977-96	-9.9	-17.7	-28.7	-5.4	-7.1	-12.0	-8.0	-16.3	-19.6
	Change in summer temperature (°C)								
1980-86	1.3	2.7	5.1	1.2	2.0	2.6	1.0	2.7	3.8
1977-96	4.1	5.5	7.9	4.0	4.8	5.4	3.8	5.5	6.6
	Percent change in summer runoff								
1980-86	-18.0	-28.5	-41.8	-12.9	-15.7	-21.0	-15.9	-23.6	-30.1

Predicted changes to seasonal runoff from the Casilian Catchment show broadly the same patterns across the three scenarios but future change compared with the reference periods may be insignificant in autumn and winter. However, the modelling suggests rainfall and total runoff to be higher in spring and much lower in summer. Using LARS-WG, all scenarios suggest that present spring rainfall (i.e. 2011–17) should be ~20% higher than in 1980–86 or ~8–10% higher than 1977–96, and that present summer rainfall should be ~10% lower than in 1980–86 and 1977–96 (Table 6). A study of rainfall data from 28 synoptic stations in Iran over the period 1967–2006 found that in northern Iran rainfall changed by +0–10% annually, +10% in spring, +0–30% in summer, +0–10% in autumn and -10–20% in winter (ShiftehSome'e *et al*. 2012). The predictions for autumn and spring thus appear consistent with observations but those for summer and winter do not. However, fifteen recent AOGCM runs for a future warmer climate indicate a decrease in summer rainfall in most parts of the mid-latitudes (which include Iran), indicating a greater risk of droughts in these regions in summer (Bates *et al*. 2008, p.38).

The uncertainties associated with the prediction of future climates are well documented, not least arising from the widely varying patterns of rainfall generated by different climate models (Bates *et al*. 2008). Previous studies have explored the possible effects of climate change on water resources in Iran (Babaeian *et al*. 2007; Abbaspour *et al*. 2009; Zarghami *et al*. 2011) and elsewhere (e.g. Bae *et al*. 2008) but using outputs from only one GCM, which greatly limits the validity and usefulness of the findings. More generally, GCMs have projected that mean water vapour, evaporation, mean rainfall especially mean annual rainfall, extreme rainfall events and rainfall intensity are likely to increase in the future (Karl *et al*. 1996, SWCS 2003, IPCC 2007, Zhang *et al*. 2009). Indeed, a small increase in mean annual rainfall that has been observed worldwide during the 20th century has been the result of heavy rainfall events (Easterling *et al*. 2000, Nearing *et al*. 2005, Rahimzadeh 2009). For example, Karl and Knight (1998) and Groisman *et al*. (2001) reported an increase by 10% from 1910 to 1996 over the United States with 53% of this increase arising from 10% of precipitation events (i.e. the most intense rainfall) (Nearing *et al*. 2005).

Drought and flooding are the two high risk Iranian weather conditions. The predicted decrease in summer rainfall and higher evapotranspiration (due to higher temperatures) can be expected to cause a reduction in the soil water and groundwater recharge. Indeed, even with higher mean rainfall, there may be less groundwater recharge if the rain falls primarily during high intensity convective events that generate surface runoff rather than infiltrating into the soil. Thus, any water management plans for northern Iran must take account of both types of hazard, such as an integrated proposal that floodwater arising from higher spring rainfall should be stored using different methods including ground water recharge systems and recharge ponds (Sharifi *et al*. 2012) to increase the availability of water during drought periods.

Irrespective of the seasonal patterns, Figure 3 suggests that whichever scenario applies, the frequency of “extreme events” in the Casilian Catchment (i.e. >18 mm d^{-1}) will increase compared with the baseline period. In general, more frequent extreme events in the future can be expected to result in more flooding events for any catchment at any time of year (Abbaspour *et al*. 2009), particularly in the form of “flash floods” and often related rainfall-induced hazards such as debris flows and other types of landslides. Detailed hazard and risk assessment exercises will be needed in order to devise appropriate strategies for minimising and mitigating the impacts of these types of events. Typical strategies may include hazard zonation, for example, preventing further development in high risk locations, and updating infrastructure specifications such as larger culverts and bridge spans to accommodate higher discharges and reduce accumulation of floodwater upstream of such structures. As always, the implementation of such strategies is likely to depend on perceptions of risk as well as scientific interpretations of probabilities balanced against local and regional economic and political factors including the healthy tourism industry in northern Iran.

6 CONCLUSIONS

This study suggests that future patterns of runoff from forested catchments bordering the south coast of the Caspian Sea in northern Iran will directly correspond with predicted changes in rainfall. Overall, patterns of rainfall and runoff in autumn and winter may be little different from the present, but that significantly higher rainfall and runoff may occur during spring with significantly lower rainfall and runoff in summer. The corresponding hazard scenarios are thus for higher probabilities of regional-scale flooding in spring and droughts in summer. This presents a fortuitously ideal basis for integrated water management strategies that capture and store excess spring runoff in order to mitigate the effects of possible summer droughts. However, a higher proportion of the rainfall is expected to occur as occasional high intensity events that can be expected to generate flash floods– and possibly landslides – at any time of year. Management and mitigation of these hazards will be required, particularly if the tourism industry of northern Iran is not to be adversely affected in the future.

Acknowledgements We are particularly grateful to the late J. Parvardeh, Head of the Surface Water Section in Tamab (Water Resources Researches Organization of Iran), who provided relevant catchment data to BZ and then FH over many years, and to staff of the Farim Wood Company who provided access for FH, BZ and APD to Sangdeh and Valikbon monitoring stations. We also acknowledge individuals and organisations who assisted FH with his research in Tehran: National Cartographic Centre of Iran; Geological Survey of Iran; Dr Saeed Morid (Forests, Range and Watershed Management Organisation, Tehran, and Tarbiate Modares University); Dr Rahim Salavi-Tabar (Mahab Ghodss Consulting Engineering Company); Moshanir Power Engineering Consultants; Dr Iman Babaeian (Atmospheric Science and Meteorological Research Centre, Tehran); Dr Niaz Ali Ebrahimipak (Soil and Water Research Institute, Tehran); and, in the UK, Dr Mikhail Semenov (Rothamsted Research, Harpenden).

Funding This research was funded by a scholarship from Azad University in Tehran to the first author to undertake a PhD at Kingston University, UK.

Disclosure Statement There are no financial interests or benefits arising from this work.

References

Abbaspour, K.C., Faramarzi, M., Ghasemi, S.S. and Yang, H., 2009. Assessing the impact of climate change on water resources in Iran. *Water Resources*, 45, W10434, doi: 10.1029/2008WR007615.

Babaeian, I., Najafinik, Z., Zabolabasi, F., Habibinokhandan, M., Adab, H. and Malbosi, S., 2007. Climate change investigation of Iran for 2010-2039 using downscaled output of ECHO-G climate model. *Geography and Development Iranian Journal*, 16, 135–152 (in Persian).

Bae, D.H., Jung, W. and Chang, H., 2008. Potential changes in Korean water resources estimated by high-resolution climate resolution. *Climate Research*, 35, 213–226.

Bae, D.H., Jung, W. and Lettenmaier, D.P., 2011. Hydrologic uncertainties in climate change from IPCC AR4 GCM simulations of the Chungju Catchment, Korea. *Journal of Hydrology*, 401, 90–105.

Barnett, D.N., Brown, S.J., Murphy, J.M., Sexton, D.M.H. and Webb, M.J., 2006. Quantifying uncertainty in changes in extreme event frequency in response to doubled CO2 using a large ensemble of GCM simulations. *Climate Dynamics*, 26, 489–511.

Banasik, K. and Hejduk, L., 2012. Long-term changes in runoff from a small agricultural catchment. *Soil and Water Research*, 7, 64–72.

Bates, B.C., Kundzewicz, Z.W., Wu, S. and Palutikof, J.P., eds., 2008. *Climate change and water*. Technical paper of the Intergovernmental Panel on Climate Change. Geneva: IPCC Secretariat.

Bennet, T., 1998. Development and application of a continuous Soil Moisture Accounting algorithm for the Hydrologic Engineering Center Hydrologic Modeling System (HEC-HMS). Unpublished MS thesis. University Of California (Davis).

Boyer, C., Chaumont, D., Chartier, I. and Roy, A.G., 2010. Impact of climate change on the hydrology of St. Lawrence tributaries. *Journal of Hydrology*, 384, 65–83.
Breuer, L., Eckhardt, K. and Frede, H.G., 2003. Plant parameter values for models in temperate climates. *Ecological Modelling*, 169, 237–293.
Chainuvati, C. and Athipanan, W., 2001. Crop diversification in Thailand. *In*: M.K. Papademetriou and F.J. Dent, eds. *Crop diversification in the Asia–Pacific region* [online]. Bangkok: Food and Agriculture Organization. RAP publication 2001/03. Available from: www.fao.org/docrep/003/x6906e/x6906e00.htm#contents(Accessed 15 July 2015).
Chang, J., Wang, Y., Istanbulluoglu, E., Bai, T., Huang, Q., Yang, D. and Huang, S., 2015. Impact of climate change and human activities on runoff in the Weihe River Basin, China. *Quaternary International*, 380–381,169–179.
Cunderlik, J.M. and Simonovic, S.P., 2005. Hydrological extremes in a southwestern Ontario river basin under future climate conditions/Extrêmes hydrologiques dans un basin versant du sud-ouest de l'Ontario sous conditions climatiques futures. *Hydrological Sciences Journal*, 50 (4), 631–654.
Douville, H., Chauvin, F., Planton, S., Royer, J.F., Salas-Melia, D. and Tyteca, S., 2002. Sensitivity of the hydrological cycle to increasing amounts of greenhouse gases and aerosols. *Climate Dynamics*, 20, 45–68.
Easterling, D.R., Karl, T.R., Gallo, K.P., Robinson, D.A., Trenberth, K.E. and Dai, A., 2000. Observed climate variability and change of relevance to the biosphere. *Journal of Geophysical Research*, 105 (D15), 101–114.
Fleming, M. and Neary, V.S., 2004. Continuous hydrologic modeling study with Hydrologic Modelling System (HEC-HMS). *Journal of Hydrologic Engineering*, 9(3), 175–183.
Garcı´a, A., Sainz, A., Revilla, J.A., A´lvarez, C., Juanes, J.A. and Puente, A., 2008. Surface water resources assessment in scarcely gauged catchments in the north of Spain. *Journal of Hydrology*, 356, 312–326.
Groisman, P.Y., Knight, R.W. and Karl, T.R., 2001. Heavy precipitation and high stream flow in the contiguous United States: Trends in the twentieth century. *Bulletin of the American Meteorological Society*, 82 (2), 219–246.
IPCC, 2000. *Emissions Scenarios* [N. Nakicenovic and R. Swart R, eds.] Cambridge University Press: Intergovernmental Panel on Climate Change.
IPCC, 2007. *Climate Change 2007, The Physical Science Basis. Contribution of Working Group I to the Fourth Assessment Report*. [S. Solomon, D. Qin, M. Manning, Z. Chen, M. Marquis, K.B. Averyt, M. Tignor and H.L. Miller, eds.] Cambridge University Press: Intergovernmental Panel on Climate Change.
Jiang, C., Zhang, L., Li, D. and Li, F., 2015. Water discharge and sediment load changes in China: Change patterns, causes, and implications. *Water*, 7, 5849–5875, doi:10.3390/w7105849.
Karl, T.R. and Knight, R.W., 1998. Secular trends of precipitation amount, frequency, and intensity in the USA. *Bulletin of the American Meteorological Society*, 79, 231–241.
Karl, T.R., Knight, R.W., Easterling, D.R. and Quayle, R.G., 1996. Indices of climate change for the United States. *Bulletin of the American Meteorological Society*, 77, 279–292.
Katiraie, P.S., Hajjam, S. and Irannejad, P., 2007. Contribution from the variations of precipitation frequency and daily intensity to the precipitation trend in Iran over the period 1960–2001. *Journal of the Earth and Space Physics*, 33(1), 67–83 (in Persian).
Kay, A.L., Davies, H.N., Bell, V.A. and Jones, R.G., 2009. Comparison of uncertainty sources for climate change impacts: flood frequency in England. *Climatic Change*, 92, 41–63.
Kharin, V.V. and Zwiers, F.W., 2005. Estimating extremes in transient climate change simulations. *Journal of Climate*, 18, 1156–1173.
King, L., Solaiman, T. and Simonovic, S.P., 2009. *Assessment of climatic vulnerability in the Upper Thames river catchment* [online]. London (Ontario): Department of Civil and Environmental Engineering, University of Western Ontario, Water Resources Research Report No. 64. Available from:www.eng.uwo.ca/research/iclr/fids/publications/products/66.pdf (Accessed 16 July 2015).

Kundzewicz, Z.W., Kanae, S., Seneviratne, S.I., Handmer, J., Nicholls, N., Peduzzi, P., Mechler, R., Bouwer, L.M., Arnell, N., Mach, K., Muir-Wood, R., Brakenridge, G.R., Kron, W., Benito, G., Honda, Y., Takahashi, K. and Sherstyukov, B., 2013. Flood risk and climate change: global and regional perspectives. *Hydrological Sciences Journal*, 59, 1–28.

Langhammer, J., Su, Y. and Bernsteinová, J., 2015. Runoff response to climate warming and forest disturbance in a mid-mountain basin. *Water*, 7, 3320–3342, doi:10.3390/w7073320.

Li, F., Zhang, G. and Xu, Y.J., 2014. Separating the impacts of climate variation and human activities on runoff in the Songhua River Basin, Northeast China. *Water*, 6, 3320–3338, doi:10.3390/w6113320.

Mahdavi, M., 2004. *Applied hydrology*. University of Tehran Press (in Persian).

McCuen, R.H., 1998. *Hydrologic analysis and design*. Upper Saddle River (NJ): Prentice Hall.

McEnroe, B.M., 2010. *Guidelines for continuous simulation of stream flow in Johnson County, Kansas, with HEC-HMS* [online]. Lawrence: Department of Civil, Environmental and Architectural Engineering, University of Kansas, report to Johnson County public works and infrastructure storm water management program. Available from: http://www.jocogov.org/sites/default/files/documents/PWK/continuous-simulation-with-HEC-HMS.pdf (Accessed 16 July 2015).

Nearing, M., Jetten, V., Baffaut, C., Cerdan, O., Couturier, A., Hernandez, M., Bissonnais, Y., Nichols, M., Nunes, J., Renschler, C., Souchere, V. and van Oost, K., 2005. Modelling response of soil erosion and runoff to changes in precipitation and cover. *Catena*, 61, 131–154.

Parvardeh, J., 1985. *Data and studies of surface waters*. Unpublished report of the Surface Water Section of the Water Resources Researches Organization of Iran (TAMAB). (In Persian).

Rahimzadeh, F., Asgari, A. and Fattahi, E., 2009. Variability of extreme temperature and precipitation in Iran during recent decades. *International Journal of Climatology*, 29, 329–343.

Rasoli, A., Babaeian, I., Ghaemi, H. and Zevarreza, P., 2012. Time series analysis of pressure of centre of synoptic patterns influencing the seasonal rainfall of Iran. *Geography and Development*, 27, 77–88 (in Persian).

Rawls, W.J., Brakensiek, D.L. and Saxton, K.E., 1982. Estimation of soil water properties. *Transactions of the American Society of Agricultural Engineers*, 108, 1316–1320.

Sajjad Khan, M., Coulibaly, P. and Dibike, Y., 2006. Uncertainty analysis of statistical downscaling methods. *Journal of Hydrology*, 319, 357–382.

Scharffenberg, W.A. and Fleming, M.J., 2010. *Hydrologic Modelling System HEC-HMS User's Manual*. Davis (California): US Army Corps of Engineers.

Semenov, M.A. and Stratonovitch, P., 2010. Use of multi-model ensembles from global climate models for assessment of climate change impacts. *Climate Research*, 41, 1–14.

Semenov, M. and Shewry, P.R., 2011. Modelling predicts that heat stress, not drought, will increase vulnerability of wheat in Europe. *Scientific Reports*, 1, 66.

Semenov, M.A., Brooks, R.J., Barrow, E.M. and Richardson, C.W., 1998. Comparison of the WGEN and LARS-WG stochastic weather generators in diverse climates. *Climate Research*, 10, 95–107.

Sharifi, F., Samadi, S.Z. and Wilson, C.A.M.E., 2012. Causes and consequences of recent floods in the Golestan catchments and Caspian Sea regions of Iran. *Natural Hazards*, 61, 533–550.

ShiftehSome'e, B., Ezani, A. and Tabari, H., 2012. Spatiotemporal trends and change point of precipitation in Iran. *Atmospheric Research*, 113, 1–12.

Singhal, B.B.S. and Gupta, R.P., 1999. *Applied hydrogeology of fractured rocks*. Dordrecht: Kluwer Academic.

Stahl, K., Hisdal, H., Hannaford, J., Tallaksen, L.M., van Lanen, H.A.J., Sauquet, E., Demuth, S., Fendekova, M. and Jódar, J., 2010. Streamflow trends in Europe: evidence from a dataset of near-natural catchments. *Hydrology and Earth System Sciences*, 14, 2367–2382, doi:10.5194/hess-14-2367-2010.

SWCS, 2003. *Conservation implications of climate change: soil erosion and runoff from cropland* [online]. Ankeny (Iowa): Soil and Water Conservation Society. Available from: http://www.swcs.org/documents/filelibrary/advocacy_publications_before_2005/Climate_changefinal_112904154622.pdf (Accessed 16 July 2015).
Tabari, H., Nikbakht, J. and ShiftehSome'e, B., 2011. Investigation of groundwater level fluctuations in the north of Iran. *Environmental Earth Sciences*, doi:10.1007/s12665-011-1229-z.
Trucanoa, T.G., Swilera, L.P., Igusab, T., Oberkampfc, W.L. and Pilchc, M., 2006. Calibration, validation, and sensitivity analysis: What's what. *Reliability, Engineering and System Safety*, 91, 1331–1357.
USACE-HEC, 2000. *Hydrologic Modelling System, HEC-HMS: Technical Reference Manual*. Davis (California): US Army Corps of Engineers, Hydrologic Engineering Centre CPD-74B.
USDA, 1986. *Urban hydrology for small catchments* [online].Washington D.C.: United States Department of Agriculture, Technical Release 55. Available from: http://cset.sp.utoledo.edu/~nkissoff/pdf/CIVE-3520/Modified-tr55.pdf (Accessed 16 July 2015).
Venturini, V., Islam, S. and Rodriguez, L., 2008. Estimation of evaporative fraction and evapotranspiration from MODIS products using a complementary based model. *Remote Sensing of the Environment*, 112, 132–141.
Wilby, R.L. and Wigley, T.M.L., 2002. Future changes in the distribution of daily precipitation totals across North America. *Geophysical Research Letters*, 29(7), 1135.
Zampieri, M., Scoccimarro, E., Gualdi, S. and Navarra, A., 2015. Observed shift towards earlier spring discharge in the main Alpine rivers. *Science of the Total Environment*, 503–504, 222–232.
Zarghami, M., Abdi, A., Babaeian, I., Hassanzadeh, Y. and Kanani, R., 2011. Impacts of climate change on runoffs in East Azerbaijan, Iran. *Global and Planetary Change*, 78(3–4), 137–146.
Zhan, C.S., Jiang, S.S., Sun, F.B., Jia, Y.W., Niu, C.W. and Yue, W.F., 2014. Quantitative contribution of climate change and human activities to runoff changes in the Wei River basin, China. *Hydrology and Earth System Sciences*, 18, 3069–3077, doi:10.5194/hess-18-3069-2014.
Zhang, X.C., Liu, W.Z., Li, Z. and Zheng, F.L., 2009. Simulating site-specific impacts of climate change on soil erosion and surface hydrology in southern Loess Plateau of China. *Catena*, 79, 237–242.